10th ANKARA INTERNATIONAL AEROSPACE CONFERENCE **AIAC-2019-147**
18-20 September 2019 - METU, Ankara TURKEY

A PRACTICAL TOOL FOR DETERMINATION AND OBSERVATION OF 3D WING AERODYNAMIC CHARACTERISTICS AT HIGH ANGLES OF ATTACK

Hasan Karali* and M. Adil Yukselen†
Istanbul Technical University
Istanbul, Turkey

ABSTRACT

In this study, a practical aerodynamic tool, which can calculate and show non-linear aerodynamic characteristics of three-dimensional wing, is developed to observe flow phenomena at high angles of attack. In particular, considering the success of the developed mathematical model in predicting pre- and post-stall aerodynamic behavior, some additions have been made which may be important in wing design and analysis stages. In this way, it is possible to calculate and visualize data such as surface pressure and velocity distribution, flow separation points, lift distribution, as well as aerodynamic performance coefficients of a wing in milliseconds on personal computer. Specifically, the program provides information on the effectiveness of the control surfaces at high attack angles by determining the flow separation points of the various wing geometries. The developed program stands out as a quick and practical tool in the early design stages. Thanks to the visualizations, this program will be very advantageous for both engineering education and R&D projects.

INTRODUCTION

Visualization has great benefits in understanding physical events. For this reason, in many scientific fields, it has been preferred to visualize an event to be investigated in an experimental setting. The biggest challenge for the test environment is its difficult and expensive installation and operation. However, with the rapid development of computers since the 1960s, it has become easier to solve physical problems at various levels. Especially after the 1990s, with the development of personal computers and programming languages, it has become possible to solve the mathematical model of many problems in any environment, convert numerical results into graphics and similar visual tools, create visualizations and animations by using graphical interfaces of computers.

In aerodynamics education, it can be difficult for the students to understand the relationship between two-dimensional and three-dimensional flow. In addition, in some design studies, the behavior and flow characteristics of the wing in high angles of attack, especially in the stall region, is a matter of curiosity. It is possible to calculate the performance coefficients and visualize the flow characteristics

*Res. Assist. in Aeronautical Engineering Department, Email: karalih@itu.edu.tr
†Prof. in Aeronautical Engineering Department, Email: yukselen@itu.edu.tr

of the wing in these regions by using computational fluid dynamics programs such as Fluent and OpenFOAM. However, these tools are not practical in terms of the computational power and time requirement [Cummings et al., 2015]. Low-order potential methods can partially meet these needs in the linear zone [Katz and Plotkin, 2001]. Programs such as XFLR5, Tornado VLM and OpenVSP, developed by various institutions or individuals, stand out as a fast, practical and inexpensive tool with the potential methods they use (Figure 1). However, these type programs can usually only perform linear region calculations. Yükselen has developed various codes to simulate aerodynamics problems for use in aerodynamic education, and presented some of them in academic publishings [Yukselen, 2012, 2014 and 2015]. In an unpublished study, he developed also a simulation code applying lifting line method to visualize the pressure distribution on a wing and its variation with geometry and angle of attack. But this code is, again, works at low and moderate angles of attack.

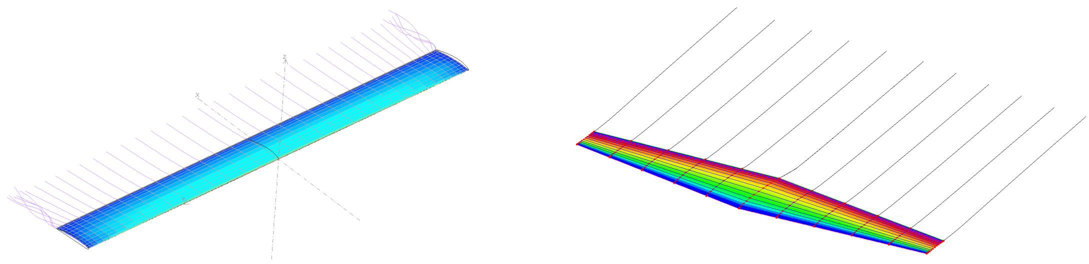

(a) (b)

Figure 1: Wing model examples of computational aerodynamic programs: (a) XFLR5 and (b) OpenVSP

In this paper, a code is presented to simulate and visualize typical characteristics of a 3D wing (Figure 2) at pre- and post-stall regimes by using our previously developed non-linear lifting line method [Karali and Yukselen, 2018; Karali, Yukselen and Inalhan, 2019]. We expect that this tool can be useful in both engineering education and R&D projects.

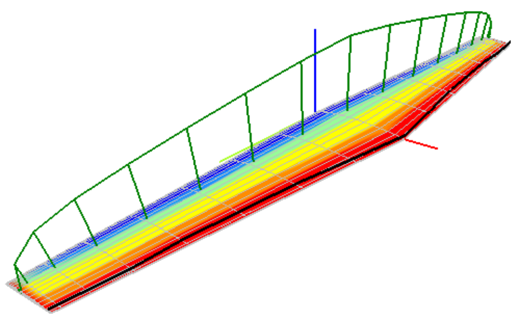

Figure 2: Wing preview of developed code with pressure contours, lift distribution (green) and flow seperation (black)

In the following sections first an outline of the non-linear lifting line method is given, then some information about the simulation code is demonstrated, and finally some applications are presented.

NON-LINEAR LIFTING LINE METHOD

In this method, potential flow based Prandtl's Lifting Line theory (also known as Linear Lifting Line theory) is modified for calculation of non-linear aerodynamic characteristics at high angles of attack [Karali and Yukselen, 2018]. The basis of the method is a partial-linear approximation to the two-dimensional lift curve with an iteration process to correct error due to linear approximation. Basic method gives lift and induced drag coefficients of a single lifting surface. Spanwise lift distribution, effective angles of attack and downwash for each station on the wing are also provided. In addition, viscous drag and pitching moment coefficients are obtained by using 2D data of wing sections. This mathematical model was extended for the complete analysis of an unmanned aerial vehicle which has multiple lifting surfaces [Karali, Yukselen and Inalhan, 2019]. However, in the scope of this study, only a single wing is considered in the developed tool.

In Prandtl's classical lifting line theory the flow around a finite wing is represented by an infinite number of horseshoe vortices in a uniform parallel free flow. A detailed information about this model can be found in any aerodynamics textbook [Anderson, 2010]. In general applications of the model, spanwise variation of strength of the bound vortex is represented by a sinus Fourier series,

$$\Gamma(\theta) = 4sV_\infty \sum_{j=1}^{N} A_j sin(j\theta) \tag{1}$$

and the aerodynamic characteristics of the wing are obtained as follows:

$$C_L = \pi ARA_1 \tag{2a}$$

$$C_{D_i} = \frac{C_L^2}{\pi AR}(1+\delta); \qquad \delta = \sum_{j=2}^{N} j\left(\frac{A_j}{A_1}\right)^2 \tag{2b}$$

$$\varepsilon = \sum_{j=2}^{N} \frac{jA_j sin(j\theta)}{sin(\theta)} \tag{2c}$$

A_j Fourier coefficients in these equations depend on the wing geometry and angle of attack. The procedure used to obtain the Fourier coefficients will not be repeated here; nonetheless, it can be found in the textbooks [see for example, Anderson, 2010; Katz and Plotkin, 2001].

In non-linear lifting line method, a partial linear approach is used to lift curve. For a spanwise station, i, of a wing at any incidence, let α_i^k and $c_{l_i}^k$ be the local geometric angle of attack and the local lift coefficient, respectively, in the non-linear region of a lift curve (see Figure 3). Assume that the lift curve slope remains constant for a small increase of $\Delta\alpha$ in angle of attack. Let α_i^{k+1} and $c_{l_i}^{k+1}$ be the new local geometric angle of attack and the local lift coefficient, respectively. As in Prandtl's classical approximation, if an equivalent 2D flow is considered for this wing section at these two geometric angles of attack, following equation can be written:

$$c_{l_i}^{k+1} = c_{l_i}^k + a_{\infty_i}^k \left[\Delta\alpha - \left(\varepsilon_i^{k+1} - \varepsilon_i^k\right)\right] \tag{3}$$

Where $a_{\infty_i}^k$ is 2D lift curve slop of this wing section around the geometric angle of attack α_i^k, ε_i^k and ε_i^{k+1} is downwash angle at α_i^k and α_i^{k+1} respectively. This equation can be written in terms of circulations as follows:

$$\frac{2\Gamma^{k+1}}{V_\infty c_i} = \frac{2\Gamma^k}{V_\infty c_i} + a_{\infty_i}^k[\Delta\alpha - (\varepsilon_i^{k+1} - \varepsilon_i^k)] \tag{4}$$

By using Eq. (1) in Eq. (4) and applying this equation for properly distributed N sections along wingspan, following linear equation system is obtained:

$$\sum_{j=1}^{N} D_{ij}^k A_j^{k+1} = \sum_{j=1}^{N} D_{ij}^k A_j^k + \Delta\alpha \qquad i = 1, 2, ..., N \tag{5}$$

where,

$$D_{ij}^k = \left(\frac{1}{\mu_i^k} + \frac{j}{sin(\theta_i)}\right) sin(j\theta_i) \qquad \mu_i^k = \frac{8s}{a_{\infty_i}^k c_i} \tag{6}$$

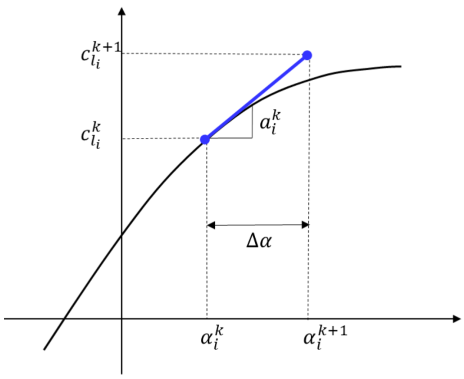

Figure 3: Partial-linear approach to the lift curve

System of Eq. (12) can be written briefly in a matrix form

$$[D_{ij}^k]\{A_j^{k+1}\} = [D_{ij}^k]\{A_j^k\} + \{\Delta\alpha\} \tag{7}$$

and resolved as

$$\{A_j^{k+1}\} = \{A_j^k\} + [D_{ij}^k]^{-1}\{\Delta\alpha\} \tag{8}$$

Thus, if A_j^k, Fourier coefficients are known at any geometric angle of attack α_i^k, it is possible to calculate A_j^{k+1} coefficients at α_i^{k+1}. This procedure begins by calculating the coefficients at zero lift angle of attack of the wing. At every new angle of attack, aerodynamic properties of the wing such as effective angle of attack,and lift coefficient, induced drag coefficient etc. can be calculated by using new A_j^{k+1} coefficients.

Note that, at each new angle of attack, the effective angles of attack and 2D lift curve slope,$a_{\infty_i}^k$, and therefore, the D_{ij}^k coefficients will change. However, before aerodynamic coefficient calculation these Fourier series coefficients are corrected via two-dimensional data.
Since the lift curve slopes are assumed to be remain constant in Eq. (6), Fourier coefficients calculated for the new angle of attack have an error depending on the step size $\Delta\alpha$. However, with the iteration process, which is shown with red dashed line in Figure 4, this error is reduced to a minimum value.

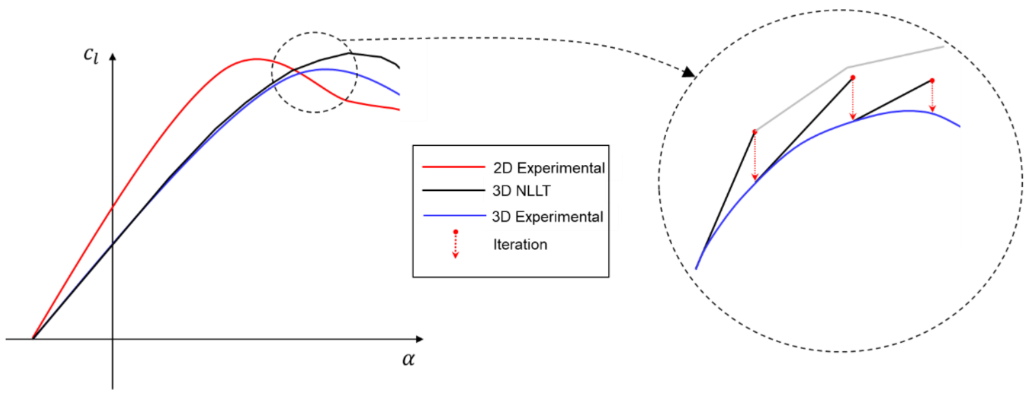

Figure 4: Iteration process representation on lift curve

The iterative method used in the current non-linear lifting line method is based on the correction of the spanwise circulation distribution by using wing section's 2D lift coefficients obtained from experiment or numerically. This procedure begins with the wing lift coefficient obtained at the new angle of attack.

The iteration steps are as follows:

1- Calculate circulation distribution by using the Fourier coefficients obtained from partial-linear approximation

$$\Gamma_i^{old} = 4sV_\infty \sum_{j=1}^{N} A_j \sin j\theta_i \tag{9}$$

2- Calculate the downwash angles by using the Fourier coefficients in Eq. (2c) and the effective angles of attack as following:

$$\alpha_{e_i} = \alpha_i - \varepsilon_i \tag{10}$$

3- For each section, determine the local lift coefficient by using the effective angles of attack in the section's 2D data obtained experimentally or numerically

4- Calculate new circulation distribution with the following relationship obtained from Kutta-Joukowski law for lift and the lift coefficient definition

$$\Gamma_i^{new} = \frac{1}{2} V_\infty c_i c_{l_i} \tag{11}$$

5- Compare these circulations with the previous one. If the difference is smaller than 10-5 exit the iteration loop, otherwise calculate new circulation values as following

$$\Gamma_i = \Gamma_i^{old} + RF\left(\Gamma_i^{new} - \Gamma_i^{old}\right) \tag{12}$$

where RF is a relaxation factor and its value is chosen as 0.05 here in the applications

6- Multiplying each side of Eq. (1) with $\sin k\theta$ and integrating for $\theta = 0$ to π one obtains

$$A_k = \frac{1}{2sV_\infty \pi} \int_0^\pi \Gamma(\theta) \sin k\theta d\theta, \quad k = 0, 1, 2, 3, \ldots, N \tag{13}$$

Calculate new A_k Fourier coefficients by using the circulation distribution in these integrals. Note that these integrals can be calculated numerically. In this study the following linear integration formula is used

$$A_k = \frac{1}{2sV_\infty \pi} \sum_{j=1}^{N} \frac{f_{j-1} - f_j}{2} \Delta\theta \tag{14}$$

8- Repeat the steps from 1 to 7 until convergence is obtained.

The non-linear lifting line method gives lift and induced drag coefficients directly. The viscous drag and the pitching moment coefficients can be obtained by using 2D experimental (or numerical) data of the wing section. For this purpose, first the 2D data is interpolated to obtain corresponding values for the effective angles of attack given by the method at each span wise section. Then these values are integrated numerically along the span.

$$C_{D_v} = \frac{2}{S} \sum_{i=1}^{N} S_i \bar{c}_{D_{v_i}}; \quad S_i = \frac{c_i + c_{i+1}}{2} (y_{i+1} - y_i); \quad \bar{c}_{D_{v_i}} = \frac{c_{D_{v_i}} + c_{D_{v_{i+1}}}}{2} \tag{15}$$

$$C_{M_y} = \frac{2}{S} \sum_{i=1}^{N} S_i \bar{c}_i \bar{c}_{m_{y_i}}; \quad \bar{c}_i = \frac{c_i + c_{i+1}}{2}; \quad \bar{c}_{m_{y_i}} = \frac{c_{m_{y_i}} + c_{m_{y_{i+1}}}}{2} \tag{16}$$

Similar to these coefficients, flow separation points and pressure coefficients also can be calculated by using two-dimensional data of the wing section. The data in the look-up table is interpolated according to the effective angle of attack at each spanwise station.

Detailed validation studies have been conducted in previous publications on this method. However, an exemplary test study is also presented here to demonstrate the capacity of the method.

In this test study, a comparison was made with the experimental results in the literature for a wing [Ostowari and Naik, 1985], whose geometric parameters and flow conditions are given in Table 1.

Table 1: Test Case geometry and flow condition

Airfoil	Planform	AR	Reynolds Number
NACA 4412	Rectangular	9	$0.25{\cdot}10^6$

It can be seen from Figure 5 that the numerical result is almost 1-1 coincident with the experimental data in both linear and non-linear regions. Non-linear behavior of the experimental lift curve starts at nearly $10°$ of attack. The maximum lift coefficient obtained numerically is very close to the experimental value.

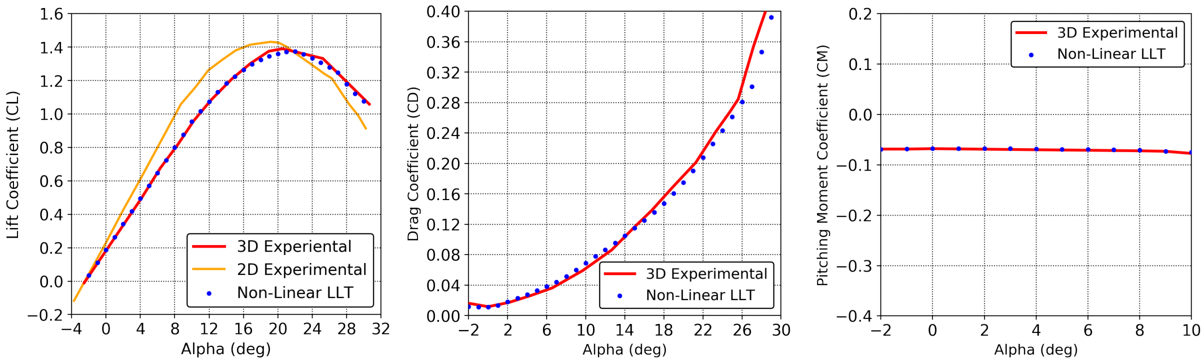

(a) (b) (c)

Figure 5: Comparison with the experimental results: (a) Lift (b) Drag (c) Pitching Moment

As previously mentioned, the methods based on lifting line theory give the induced drag coefficients directly. The viscous drag and pitching moment also can be calculated from the two-dimensional data by a simple approach outlined before. The total drag and pitching moment coefficients obtained by this way are presented in Figure 5 (b) and (c) as compared with the experimental data. The numerical results are generally very close to the experimental data.

These results show that the Non-Linear Lifting Line Method can accurately calculate aerodynamic performance at both linear and non-linear region up to $5 - 10°$ beyond the stall point.

COMPUTER PROGRAM FOR NON-LINEAR AERODYNAMICS

A computer program in Visual Basic language was developed to be used as a part of computer assisted aerodynamics education and R&D projects applying our non-linear lifting line method for the aerodynamic analysis of 3D wing and OpenGL library for visualizations. By using its interface, it is possible to generate a wing and analyse/visualize its performance in split-seconds.

The code calculates primarily lift and induced drag coefficients and downwash angles for spanwise wing sections by using non-linear lifting line method, as described in previous section. Then, it calculates viscous drag and pitching moment coefficients, and chordwise pressure distributions on each spanwise stations, by using effective angles of attack at each spanwise sections with 2D airfoil data. Two-dimensional data is inserted into the program via tables created by using the results of other programs such as XFOIL [Drela, 1989] or CFD codes or data obtained experimentally. At the same time, spanwise lift distribution at any angle of attack is an output of the program. Furthermore, flow separation points are also calculated via effective angle of attack.

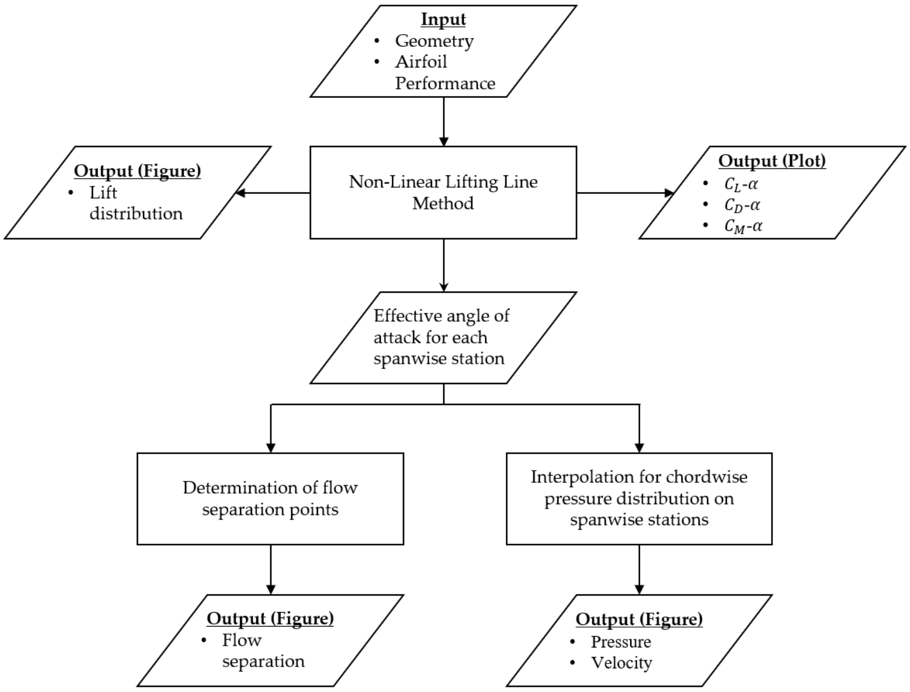

Figure 6: Flow chart of computer program

The main structure of the program is shown schematically in Figure 6. A simple and handy interface has been developed for this program using Visual Studio 2019 (Figure 7). In the inputs section, the geometrical data of the wing can be entered and the parameters to be displayed related to the flow can be selected. As a result of the analysis, the wing is drawn in 3D and given in the interface so that it can be controlled with the mouse. In addition, the aerodynamic performance of the wing is given as a plot. Outputs section shows aerodynamic coefficients for chosen angle of attack. The log file shows the total calculation time and the number of iterations.

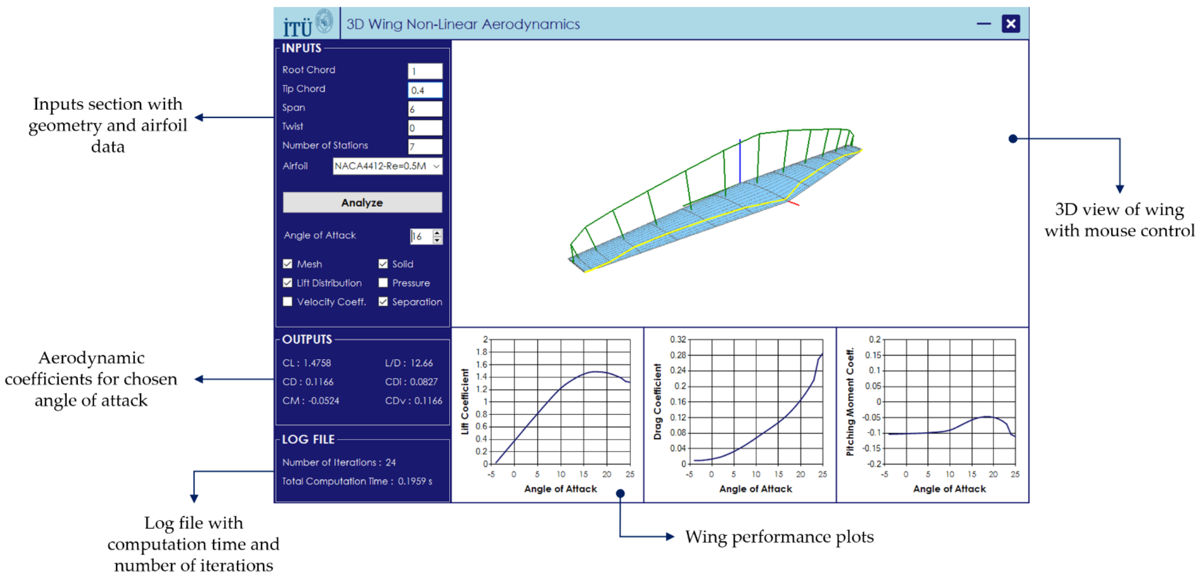

Figure 7: GUI of 3D Wing Non-Linear Aerodynamics program

Mesh/Solid drawing options make it possible to visualize the wing according to the given inputs. Both drawing options can be used alone or in combination. Flow separation option combines the calculated separation points at the spanwise stations. On the upper surface of the wing, the yellow line represents the separation line which changes with the angle of attack. Similarly, lift distribution is shown with a green curve on the vertical axis of the wing (Figure 8).

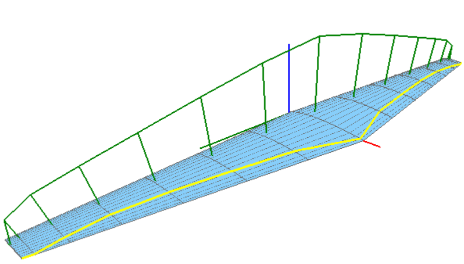

(a)

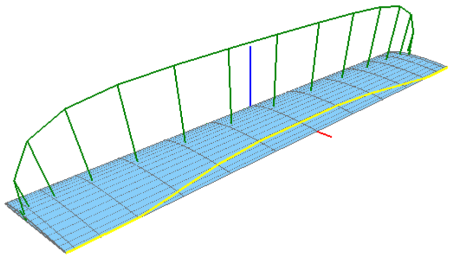

(b)

Figure 8: Flow separation and lift distribution on wings: (a) Tapered (b) Rectangular

In addition, it is possible to plot chordwise velocity distributions of the lower and upper surfaces at spanwise stations. This graph clearly illustrates the cause of the performance difference of the wing sections along the span and shows the relationship between two- and three-dimensional flow (Figure 9).

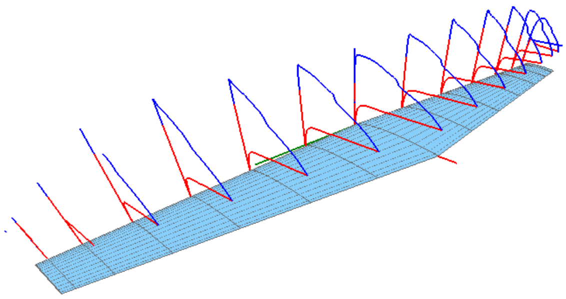

Figure 9: Chordwise velocity distribution along span

Finally, the pressure drawing option allows to display the pressure contours of upper and lower surface. The transition from low to high pressure is represented by the color change from blue to red, respectively (Figure 10).

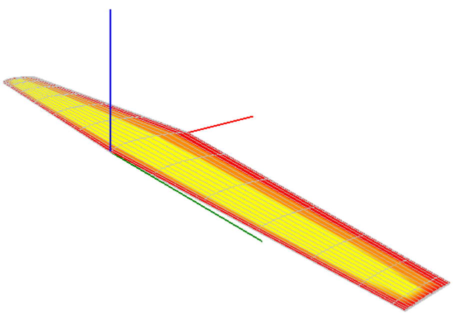

(a)

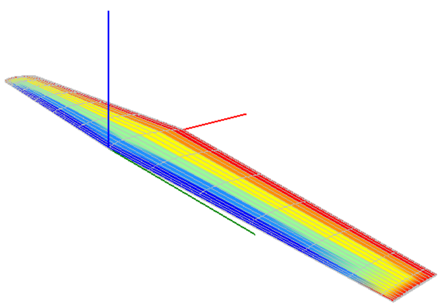

(b)

Figure 10: Pressure contours on tapered wing: (a) $\alpha = 0°$ (b) $\alpha = 10°$

APPLICATION OF THE METHOD

In this section, the results of test application of the current mathematical model are presented to show its applicability, limits, advantages and disadvantages. The aerodynamic database in the literature [Petrilli et al., 2013], which was created with intense computational fluid dynamics tool NASA TetrUSS USM3D to determine the performance of the wings at stall and post-stall angles of attack, is used for comparison.

A rectangular wing of $AR = 12$ with NACA 4415 section is used for this application. Specifications for wing and flow are given in Table 2.

Table 2: Wing geometry and flow condition

Airfoil	Planform	AR	Reynolds Number	Mach Number
NACA 4415	Rectangular	12	$3.0{\cdot}10^6$	0.2

In Figure 11a, orange dashed line and red line represents, respectively, the two- and three-dimensional data obtained from NASA TetrUSS USM3D tool. Developed method represented with blue dots in the same figure. The numerical result is almost 1-1 coincident with the validation data in both linear and non-linear regions. The maximum lift coefficient and stall angle of attack obtained numerically are very close to the validation value. In the Figure 11b, section lift coefficients, which are calculated and visualized by developed method, are compared with CFD results. Considering that non-linear behavior starts at 12°, the calculated lift distribution at the pre-stall angle of attack ($\alpha = 14°$) appears to be very successful. It is important to note that the method calculates these values at a low number of stations. This is why the straight lines connecting these points remain rough.

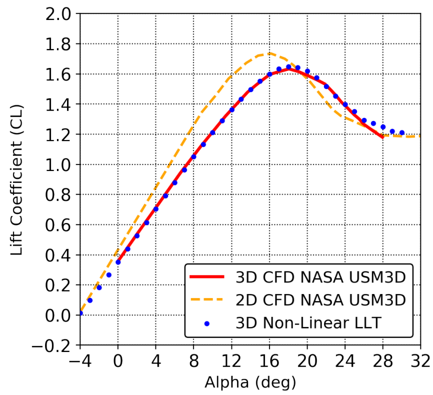

(a)

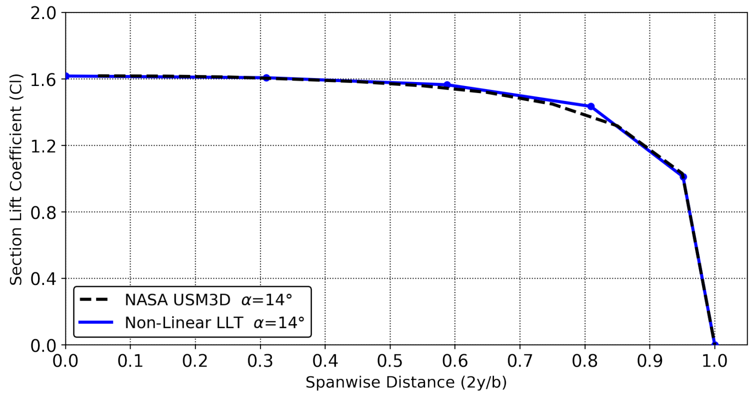

(b)

Figure 11: (a) Wing lift curves obtained from literature and code (b) Lift distribution at pre-stall

Figure 12 gives a direct comparison between the results of current method and NASA USM3D CFD tool in terms of section lift coefficient distribution at stall and post-stall. Non-Linear Lifting Line method predicts the lift distribution with a very small error margin at stall angle of attack, which is represented with red line. Furthermore, it can calculate general characteristics of lift distribution at post-stall region correctly. As can be seen from the curve indicated with orange, large fluctuation in the lift distribution can be captured by developed method. However, low ones between spanwise stations are ignored by the program. Nevertheless, the data obtained from a program that calculates all angles of attack range in the 0.1 second calculation time is quite satisfactory.

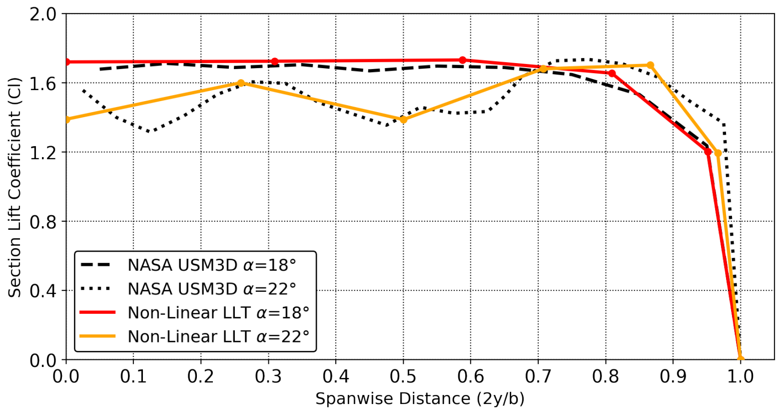

Figure 12: Semi-wing section lift distribution at stall and post-stall region

The flow separation lines, which is another feature calculated by the developed method and visualized on the wing, are compared with the results in the database. For this purpose, the required two-dimensional flow separation input was obtained by using XFOIL. The results are shown in the Figures 13, 14 and 15 which are formed as scaled half-wing. In the graphs, the same color was used for the angles of attack as in the previous ones.

According to the lift curve in Figure 11a, wing stall begins at 18° angle of attack. It is known generally that for a rectangular planform, first the wing's root region stalls. This situation can be observed also in the results of the numerical analysis and CFD. Similar to the lift distribution, the method was also able to capture large changes in flow separation points at the spanwise stations. The results were found to be quite successful for a low order method.

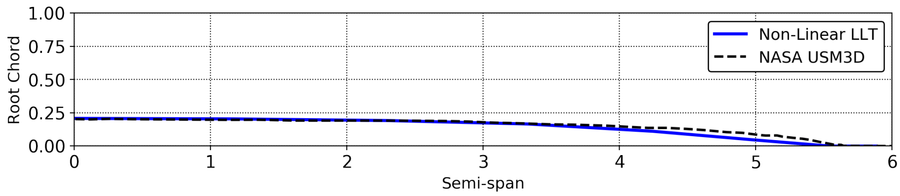

Figure 13: Flow separation at pre-stall ($\alpha = 14°$)

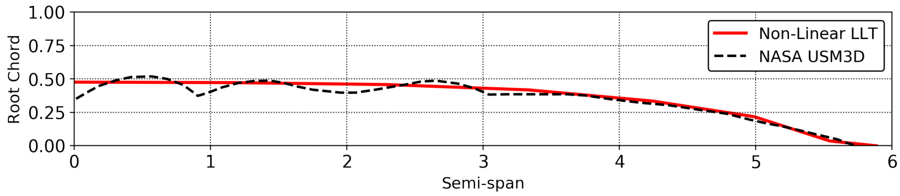

Figure 14: Flow separation at stall ($\alpha = 18°$)

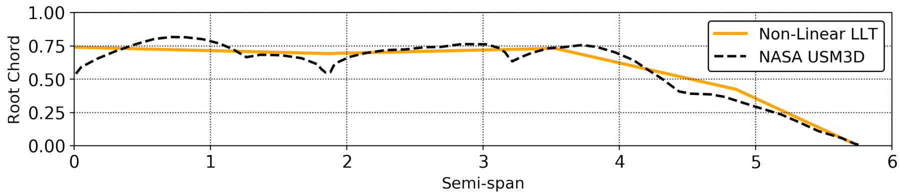

Figure 15: Flow separation at post-stall ($\alpha = 22°$)

CONCLUSIONS AND FUTURE WORK

In aerospace engineering, there is always a need for a fast and reliable tool to determine aerodynamic performance of lifting surfaces. These tools are especially useful in conceptual and preliminary design phases of R&D projects. In addition, programs with visualizations have become an indispensable part of engineering education in the modern era.

Thanks to the developed program, it is possible to calculate and visualize the aerodynamic performance and flow characteristics of a wing in a wide range angle of attack in sub-seconds. Pressure and lift distributions, flow separation on the wing at pre- and post-stall became visible. Thus, it is possible to observe the flow on the wing and control surfaces. The calculated data were validated by comparing with the results of NASA TetrUSS USM3D CFD tool. It was found that the method can accurately calculate the flow behavior as well as the aerodynamic performance coefficients. These validation studies prove that iteration process not randomly converged to find aerodynamic coefficients at post-stall region.

It has been shown in previous published studies that the method can calculate aerodynamic performance coefficients for the wing-tail combination. By simply integrating these into the existing improved interface, it is possible to make the improvements and visualizations mentioned in this paper for the wing-tail configurations.

References

Anderson Jr, J. D. (2010) *Fundamentals of aerodynamics*, Boston: McGraw-Hill Education

Cummings, R. M., Mason, W. H., Morton, S. A., & McDaniel, D. R. (2015) *Applied computational aerodynamics: A modern engineering approach*, Cambridge University Press

Drela, M. (1989) *XFOIL: An analysis and design system for low Reynolds number airfoils*, Springer, Berlin, Heidelberg

Karali, H. and Yukselen, M. A. (2018) *Üç Boyutlu Kanat Aerodinamik Özelliklerinin Non-Lineer Analizi*, VII. Ulusal Havacilik ve Uzay Konferansi, Sep 2018

Karali, H., Yukselen, M. A. and Inalhan, G. (2019) *A New Non-Linear Lifting Line Method for 3D Analysis of Wing / Configuration Aerodynamic Characteristics with Application to UAVs*, AIAA Scitech 2019 Forum (p. 2119), Jan 2019

Katz, J. and Plotkin A. (2001) *Low-speed aerodynamics*, Cambridge University Press

Ostowari, C. and Naik, D. (1985) *Post-stall wind tunnel data for NACA 44xx series airfoil sections*, Texas A. and M. Univ., College Station (USA), Dept. of Aerospace Engineering

Petrilli, J. L., Paul, R. C., Gopalarathnam, A., & Frink, N. T. (2013) *"A CFD database for airfoils and wings at post-stall angles of attack*, 31st AIAA Applied Aerodynamics Conference (p. 2916)

Yukselen, M. A. (2012) *Computer Assisted Aerodynamics Education*, Procedia - Social and Behavioral Sciences

Yukselen, M. A. (2014) *Havacılık, Uçak ve Uzay Mühendisliği Eğitiminde Bilgisayar Desteği*, V. Ulusal Havacilik ve Uzay Konferansi, Sep 2014, Kayseri

Yukselen, M. A. (2015) *Uçak Ön Tasarımında Konfigürasyon Aerodinamiğinin Yeri ve Bilgisayar Desteği*, FİGES, XIX Bilgisayar Destekli Sistem Modelleme Konferansi, Apr 2015, Ankara